

## Energy management system for AC/DC HMGS integrated with interconnected renewable sources and interlinking converter

Syed Abdul Razzaq, Vairavasamy Jayasankar

Department of Electrical and Electronics Engineering, Vel Tech Rangarajan  
Dr. Sagunthala R and D Institute of Science and Technology, Chennai, India

### Article Info

#### Article history:

Received Oct 23, 2022

Revised Dec 7, 2022

Accepted Dec 23, 2022

#### Keywords:

Battery management system

Droop control

Energy management system

Interlinking converters

### ABSTRACT

AC/DC hybrid micro grid system (HMGS) is designed with renewable energy sources (RES) and battery energy storage system (BESS) with unique control schemes, interfaced with multi terminal interlinking converters (ILCs). This ILC operates on droop control scheme to guarantee bidirectional power sharing to AC/DC sub grids. The power sources in AC/DC sub grids like PV, Fuel cell, BESS are controlled by advance control methods for maximum power extraction with power quality. A three-level control structure is designed for optimal energy management system (EMS). The first level confirms the power balance in AC/DC sub grid with autonomous bidirectional power transfer via ILC in islanded mode. The second level tracks the batteries state of charge (SoC), based on the minimum and maximum SoC the battery operates for charging and discharging. The third level gives the power redundant capability for critical loads connected in AC/DC sub grid for DC system and single-phase system.

*This is an open access article under the [CC BY-SA](https://creativecommons.org/licenses/by-sa/4.0/) license.*



### Corresponding Author:

Syed Abdul Razzaq

Department of Electrical and Electronics Engineering

Vel Tech Rangarajan Dr. Sagunthala R and D Institute of Science and Technology

No. 42, Avadi-Vel Tech Road Vel Nagar, Avadi, Chennai, Tamil Nadu 600062, India

Email: vtd516@veltech.edu.in

## 1. INTRODUCTION

Various components in micro grid (MG) are discussed with a conventional droop control for AC/DC hybrid micro grids system (HMGS) with an unique protection system [1]. For renewable energy sources (RES) integrated in HMGS, a strategic model is designed for defining the probabilities for delivering active and reactive power [2]. A review paper discusses in detail about the control techniques for AC/DC HMGS [3]. Small signal model is developed for back to back converters and equally valid for large connected MG [4]. An algorithm is designed with adaptive model and predictive control to maintain the operational costs and improve the system efficiency with a unique energy management system (EMS) [5]. A hierarchical structure is designed for control of DC bus voltage, to increase the reliability and efficiency with primary, secondary and tertiary controls [6]. Improved particle swarm optimization is used to improve the system dynamics with master and slave controls for RES with interlinking converter (ILC) connected to MG [7].

A detailed analysis on DC-MG is elaborated for energy saving in DC distribution system [8]. Stability issues while sharing optimal power through AC/DC grids and restoring the frequency by highlighting the stable and unstable droop gains in root locus are discussed [9]. A dual droop control is suggested with virtual synchronous machine for reducing the impact of circulating currents and the harmonics generated due to connection of anti-parallel diodes is analyzed [10]. The control scheme is derived for battery energy storage system (BESS) and wind energy for optimal usage in MG [11]. A novel scheme is

designed for hybrid AC-DC MG for optimal power transfer with six switch AC/DC converter combined with DC/DC unidirectional full bridge converter [12]. Load sharing in MG with parallel connected inverters is discussed with the communication link based control [13]. A decentralized technique is designed for islanded mode of MG for uniformly power sharing and improve the overall power quality [14]. A droop based control scheme is designed to control the frequency and voltage for off-grid MG [15].

In the current trends DC system is also treated as main grid with huge power delivering capacity with an advantage of power injection to load and grid. With the tremendous outcomes of bidirectional power converter for AC/DC grids which is ILC, the use of distributed generation (DG) and energy storage system (ESS) are interconnected with multi-port ILC to form a reliable, robust and efficient MG. ESS performance depends on the state of charge (SoC). Hence, the goals with ESS can set for the performance of MG. Clustering the bidirectional power flow, SoC, maximum power point tracking (MPPT) a hierarchical control scheme can be designed for optimal power flow with robust and redundant power in MG.

## 2. AC/DC HMGS MODELLING AND CONFIGURATION

The proposed AC/DC HMGS is connected with multiple ESS and DG which are interfaced with multi-port ILCs for demand-based power flow in the sub grids. During islanded mode the grid power is disconnected from utility power supply via automatic or static transfer switch (ATS/STS). The proposed control schemes uniformly distribute power with optimal power management. This hierarchical scheme tracks the complete EMS of MG. DC MG can be controlled with DC bus voltage and battery SoC status. The primary, secondary and tertiary control levels are summarized as:

- Bidirectional power flow in AC/DC sub grids by voltage and frequency droop controls
- Continuous tracking of ESS and DG like batteries, photovoltaic (PV), wind
- Universal power sharing in multiple interconnected MG based on load demand

The importance of DC distribution system is discussed for household applications is discussed in [16]. Voltage and current control scheme are designed for DC nano grid with different scenarios and the major benefits [17]. The possibility of interconnecting single phase ILC and three phases ILC in HMGS is described in [18].

### 2.1. Design of photovoltaic system

Load shedding for domestic users is quite common in rural areas, the scheme is developed for load management for PV system for maximum power utilization [19]. Sun irradiance and temperature are the main dependents for maximum PV power output, due to variations in both PV system is considered to be nonlinear. The voltage and current capacity of PV system depends on arrangement of cells in series and parallel. Figure 1 shows the PV system with DC/DC converter and its control. Number of modules connected in series is given by (1).

$$M_{series} = 0.5 \frac{V_{dc}}{V_{max}} \quad (1)$$

Where  $M_{series}$  is modules in series,  $V_{dc}$  is voltage at inverter input,  $V_{max}$  is maximum voltage from MPPT. The number of modules connected in parallel is given by (2).

$$M_{parallel} = 0.5 \left( \frac{P_{inv}}{P_{string}} \right) \quad (2)$$

DC link voltage feeding the inverter is given by (3).

$$V_{dc} \geq 2\sqrt{2} * V_{phase} \quad (3)$$

$V_{phase}$  is RMS value of inverter output voltage. PV current is given by (4).

$$I_{pv} = i_{pv} - i_0 * \left( e^{\left( \frac{q(U_{solar} + R_{series} * I_{series})}{AVT} \right)} - 1 \right) - \left( \frac{U_{solar} + R_{series} * I_{series}}{R_{parallel}} \right) \quad (4)$$

Where  $I_{pv}$  is current by PV,  $i_{ph}$  is photocurrent,  $i_0$  is diode saturation current,  $U_{solar}$  PV panel voltage,  $i_{solar}$  is output current of PV cell,  $R_{ser}$  series resistance,  $R_{par}$  parallel resistance, A is diode ideality factor, T is panel operating temperature in K<sup>0</sup>, V is Boltzmann constant ( $1.38 * 10^{-23}$ ) JK<sup>-1</sup>, q is electron charge ( $1.602 * 10^{-19}$ ).

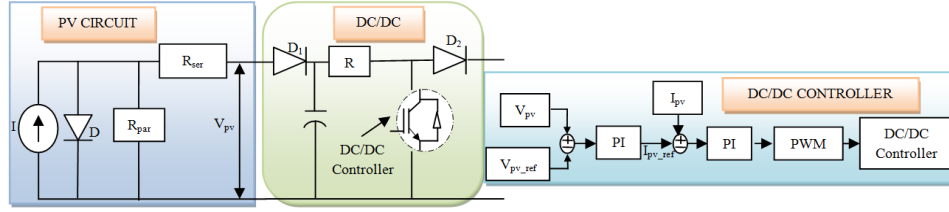


Figure 1. PV system with DC/DC converter with its control

## 2.2. Modelling of BESS

Two most famous varieties of batteries are lead-acid and lithium-ion. BESS provides a major power contribution in MG or DC power. The charging and discharging of batteries provide an option to the MG to sell the surplus power to utility grid or for electric vehicle (EV) charging. With the EMS tool the power balance and imbalance can be tracked. Whereas battery management system (BMS) can monitor the SoC, depth of discharge (DoD), each cell voltage, life, temperature and connected battery strings. The threshold values are defined for control and operation of BMS. The activation of fuel cell, super capacitor is designed based on the deficient of SoC to provide backup power for BESS connected loads. Figure 2 shows the bidirectional DC/DC converter with charging/discharging control and also SoC based control. The battery mathematical equation depends on voltage source and its internal resistance. Battery voltage is given by (5).

$$V_{bat} = V_{bat-int} - R_{int} * I_{bat} \quad (5)$$

During the state of battery charging

$$V_{bat-int} = V_{bat-open} - X_{bat} \left( \frac{C_{max-bat}}{C_{max-bat} - C_{bat}} \right) * I_{bat-ch} - X_{bat} \left[ \frac{(C_{max-bat}(\Delta_{bat-ch}))}{(C_{max-bat} - C_{bat})} \right] * C_{bat} + A_{bat} e^{-B_{bat} * C_{bat}} \quad (6)$$

During the state of battery discharge

$$V_{bat-int} = V_{bat-open} - X_{bat} \left( \frac{C_{max-bat}}{C_{max-bat} - C_{bat}} \right) * I_{bat-dis} - X_{bat} \left[ \frac{(C_{max-bat}(\Delta_{bat-ch}))}{(C_{max-bat} + 0.1C_{max-bat})} \right] * C_{bat} + A_{bat} e^{-B_{bat} * C_{bat}} \quad (7)$$

Where  $V_{bat-open}$  is open circuit voltage of battery,  $X_{bat}$  is the polarization constant,  $C_{bat}$  is current capacity of battery in Ah,  $I_{bat-ch}$ ,  $I_{bat-dis}$  is battery current during charging and discharging respectively,  $C_{bat}$  and  $C_{bat-max}$  are not equal due to various constraints.  $\Delta_{bat-ch}$ ,  $\Delta_{bat-dis}$  are binary values.  $A_{bat}$  is amplitude of the exponential term. The capacity of battery is known from (8).

$$C_{bat} = \int I_{bat} dt \quad (8)$$

Whereas SoC of battery capacity is defined by (9).

$$SoC_{bat} = \frac{C_{bat}}{C_{max-bat}} \quad (9)$$

The modeling of battery where SoC is considered as state variable. The battery discrete time is given as (10).

$$SoC_{BESS}(t_{k+1}) = SoC_{BESS}(t_k) + \frac{(\eta_{ch} P_{ch}(t_s) T_s)}{C_{BESS,r}} - \frac{P_{dis}(t_k) T_s}{\eta_{dis} * C_{BESS,r}} \quad (10)$$

Where  $P_{ch}$ ,  $P_{dis}$  is battery power charging and discharging,  $\eta_{ch}$ ,  $\eta_{dis}$  efficiency of charging and discharging,  $C_{BESS,r}$  is rated stored battery capacity in kWh.

### 2.3. SOC battery control

Control of charging and discharging of BESS using a micro controller is discussed in [20]. DC-DC bidirectional converter is used for injecting and absorbing power in BESS. The control scheme is shown below in Figure 2. Based on the difference in between nominal and reference DC voltage the result is fed to proportional integral (PI) controller. In the inner loop control PI output decides the status of charging/discharging. The condition decides the charging of battery when the nominal DC voltage is higher than reference voltage, forcing to generate negative current reference at outer loop. The change in duty cycle directs the current flow from DC bus to BESS, in the inner current loop this behavior is considered as battery charging. Due to load burden on DC bus, as a result decrease in DC bus voltage with respect to reference voltage, a positive current reference is generated. This leads to dispatch power to loads and behavior is considered as battery discharging.

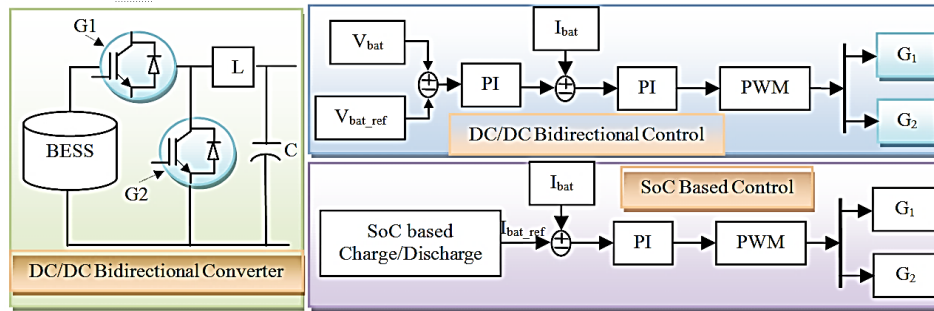


Figure 2. Bidirectional DC/DC converter with bidirectional control and SOC based control for BESS

In MG continuous monitoring and control of SoC of BESS is essential.  $I_{bat}$  minimum and maximum ranges can be set for charging and discharging of battery.  $I_{bat}$  is compared with reference values which are fed to PI controller for generating signals for current flowing.

$$\min \leq \text{SoC} \leq \max \quad (11)$$

$$-\frac{P_{bat-N}}{V_{bat}} \leq I_{bat} \leq \frac{P_{bat-n}}{V_{bat}} \quad (12)$$

Where  $P_{bat-N}$  is battery rated power, kWh and  $V_{bat}$  nominal voltage.

### 2.4. Interconnecting BESS AC power grid with ILC

A new proportional control method is discussed which uses the AC frequency to track the live power for power balancing during nonlinear loads for BESS and RES sources connected to MG [21]. A review article discusses the contributions of ILC in MG for power exchange due to load demand [22]. The demand and significance of BESS is making power system more reliable during overloading conditions. These are integrated with AC system. The real time SoC of battery is taken from BMS by coulomb counting method. The DC voltage from DC bus and frequency from AC system is used to obtain current reference in outer control loop. This scheme provides any variation in loads will drastically vary frequency and power transfers from battery. Battery DoD is identified by its stored charge. Based on the voltage variations limits the power delivering can be identified.

$$F_{ref-ac} - F_{ac} = \frac{1}{\text{SoC}} (V_{ref-dc} - V_{dc}) \quad (13)$$

$V_{dc}$  is DC bus voltage of BESS. The (13) uses battery Charge for knowing the variations in battery voltage due to load variations. BESS should be capable of delivering power at higher SoC% to loads and absorb power during below the threshold value of SOC%. For instance, the battery discharges simultaneously, which is connected to load if load increases the frequency will decrease. From (13) fall in frequency impacts on higher SoC battery making to deliver power to loads. Battery in charging mode, while loads are increased the voltage of battery decreases. Battery string with higher SoC% will transform the voltage fluctuations into minor change in frequency hence less power is delivered to refill the battery.

Similarly, smaller SoC% undergoes large frequency variation and power will be injected to BESS for sufficient charging.

### 2.5. Modelling of fuel cell

Few fuels used in the process of electrochemical for generating energy are hydrogen, hydrocarbons, oxygen flows and methanol. Fuel stack are assembled of multiple cells connected in series. Types of fuel cell are phosphoric acid, molten carbonate, solid oxide, polymer electrolyte membrane and alkali. The anode which behaves as electrode to help for separating the hydrogen gas molecules into electrons and protons. Figure 3 shows the chemical reaction of fuel cell, the final each cell voltage depends on activation, ohmic and concentration losses.



The reaction follows the protons move forward towards cathode from electrolyte.



The fuel cell reaction is given as (16).



The stack voltage is given by (17).

$$V_{FC} = N_{FC} * V_{FC} \quad (17)$$

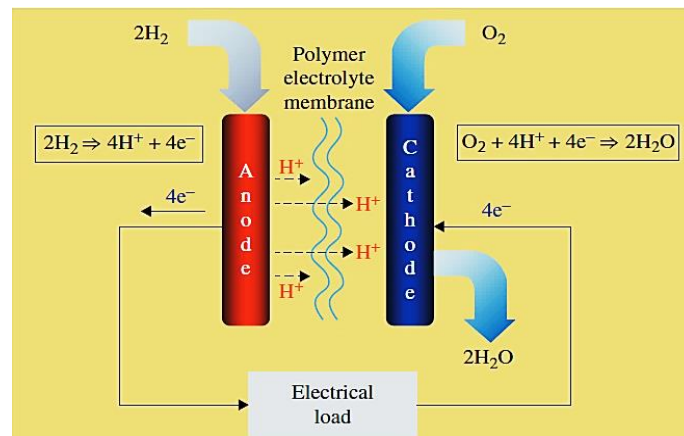


Figure 3. Basic diagram of fuel cell

### 2.6. Boost converter

The Figure 4 shows the circuit diagram of DC/DC boost converter with controller for boosting the voltage to 370 V and 800 V. The voltage step-up depends on the duty cycle (D). In detail discussion on power electronics converter is discussed with control method [23].

$$V_{out} = \frac{V_{in}}{1-D} \quad (18)$$

The output power is generated based on voltage droop as the change in load varies frequency, SoC, DC voltage.

$$\Delta V_{dc-bat} = \frac{\Delta P_{dc-bat}}{1000} \quad (19)$$

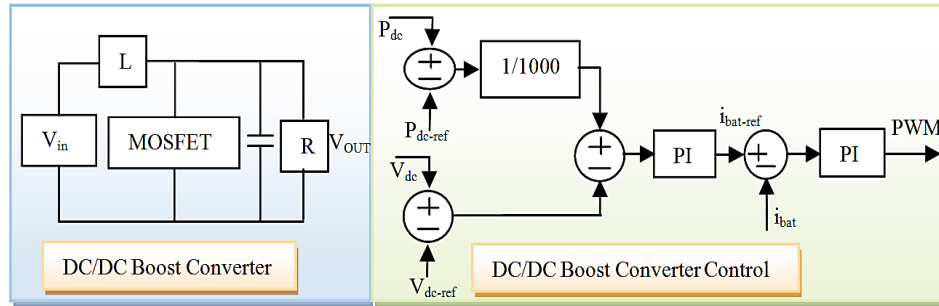


Figure 4. DC/DC boost converter with controller

## 2.7. Modelling of interlinking converter

ILC provides variety of features power transfer in AC/DC grids with control on active and reactive power in the MG, reduced circulating currents, autonomous operation. Mathematical model on AC side is given as (20):

$$U_{ilc} = V_{grid} + I_{inv}R_{filter} + L_{filter} \left( \frac{dI_{inv}}{dt} \right) \quad (20)$$

where  $U_{ilc}$  is converter voltage,  $V_{grid}$  is grid voltage,  $I_{inv}$  is inverter output current,  $R_{filter}$  is equivalent resistance and  $L_{filter}$  is filter inductance. ILC active and reactive power outputs is given as (21) and (22).

$$P = \frac{3}{2} [Re(V_{grid} * I_f)] \quad (21)$$

$$Q = \frac{3}{2} [Im(V_{grid} * I_f)] \quad (22)$$

LC filter during islanded capacitance,  $C_f$  is given as (23).

$$C_{filter} \left( \frac{dV_c}{dt} \right) = I_{filter} - I_{load} \quad (23)$$

Mathematical model of ILC can be given as (24).

$$V_i = I_{filter} * R_{filter} + L_{filter} \left( \frac{dI_{filter}}{dt} \right) V_c \quad (24)$$

## 2.8. Energy management system

A review paper discusses the polices and regulations implemented for the transactive markets and also for the load restoration in HMGS [24]. For a stable system supplying a redundant power increases the dependence of continuous power. The power flow schematic is designed for EMS. Power balance equation as an example is shown in (25) with PV and BESS as sources feeding AC/DC loads. Figure 5 shows the flow chart for EMS.

$$P_{pv} - P_{loss} = P_{ac-load} + P_{dc-load} + P_{bat} \quad (25)$$

$P_{loss}$  is total power loss in MG.

$$P_{gen-net} = P_{gen-tot} - \left( P_{ac-loads} + P_{loss} \right) \quad (26)$$

Power flow diagram is designed with PV and BESS as main power source feeding AC/DC loads with the conditions of SoC, battery charging/discharging status and overloading.

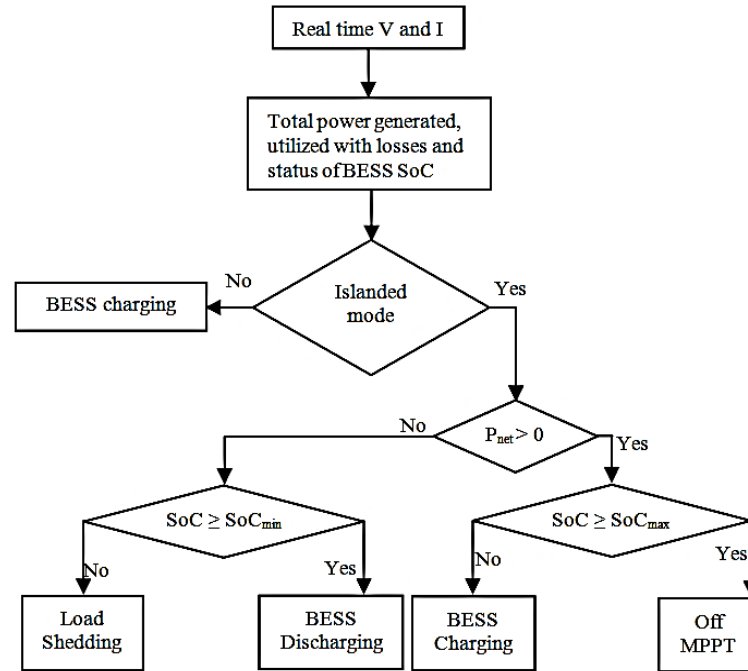


Figure 5. Flow chart for energy management system

### 3. ASSEMBLY OF AC/DC HMGS

The assembly of AC/DC HMGS is shown in Figure 6. Harmonics are major concern in electrical system, a harmonics-based droop control is designed for MG with multi power sources integrated with ILC [25]. LCL and LC filters are placed to eliminate voltage ripples and reduce current harmonics with the power quality. Large capacity capacitor is enforced at DC side to reduce the ripples. Phase locked loop (PLL) is used to obtain frequency and phase angle from AC system. Using Clarke and park transformation output voltages and currents are transformed into dq frame of axis and again applied with inverse Clarke and park transformation for dq to abc transform to feed pulse width modulation (PWM) for ILC signals. Proposed outer loop control is associated with converter power, frequency and DC voltage thus current references are obtained. PI controller is used to generate current references, these current references are fed to inner control loop basically current control segment. No reactive power at DC side hence  $i_{q-ref}$  is taken as zero.

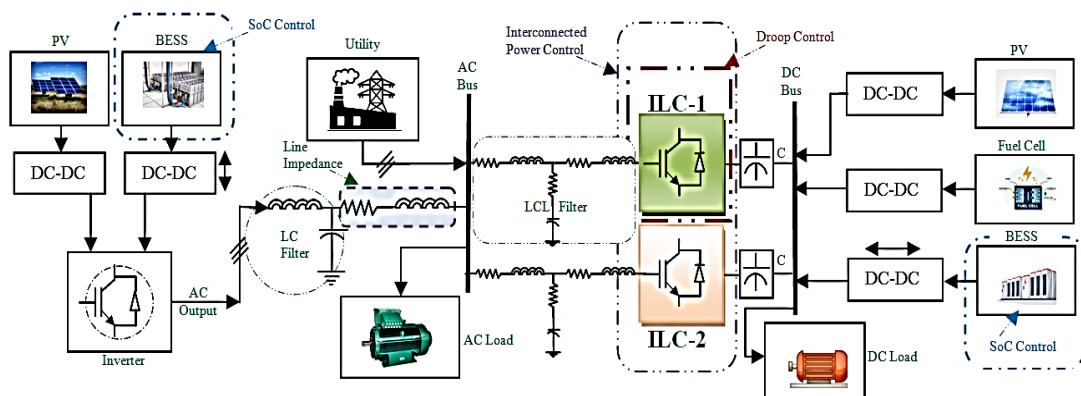


Figure 6. Proposed layout for AC/DC HMGS

### 4. CONTROL OF ILC

The various methods of droop control are discussed [26]. The proposed control scheme for ILC works on the generalized droop control. The ILC performs the power sharing upon the triggering pulse defined from the AC frequency, DC voltage and converter power. The control scheme continuously monitors



voltage with reference voltage, during the deficit of power in DC load side due to increase in loads, the voltage on DC bus decrease which changes the DC power generated the additional power is shared from AC source through ILC-1. This power is termed as positive and converter performance is a rectifier. Similarly, change in AC load side causes change in system frequency, thus impact on DC voltage is also caused. The deficit power in AC load side is shared from DC power sources via ILC-1. This power is termed as negative and converter performance is an inverter. The mathematical model of control scheme is shown in (27).

$$\lambda_1 U_{dc} + \lambda_2 P_{ilc} - \lambda_3 F - (\lambda_1 U_{dc-ref} + \lambda_2 P_{ilc-ref} - \lambda_3 F_{ref}) = 0 \tag{27}$$

Where  $\lambda_1, \lambda_2, \lambda_3$  are modulating factors with 0.3, 0.007, 10 values respectively. The change in AC generation due to load variation causing change in frequency is given by (28).

$$\sum P_{ac-gen} = \left(\frac{2\pi}{x}\right) * \Delta F \tag{28}$$

Where x is frequency droop.

$$X = \frac{F_{max} - F_{min}}{P_{ilc-ac}} \tag{29}$$

$F_{max}$  is maximum frequency, and minimum frequency is  $F_{min}$ . The change in DC power generated by source due to change in DC voltage is given by (30).

$$\sum P_{dc-gen} = \frac{\Delta V_{dc}}{y} \tag{30}$$

Where y is DC voltage droop.

The Figure 7 shows the variation in loads causes the change in DC voltage and change in frequency. The control scheme for ILC-1 is shown in Figure 8. The significance of this scheme is power is shared autonomously and bi-directionally without any communication link. ILC-2 feeds the critical and non-critical loads with single phase ILC. Voltage and current control are designed as outer and inner loop control as shown in Figure 9.

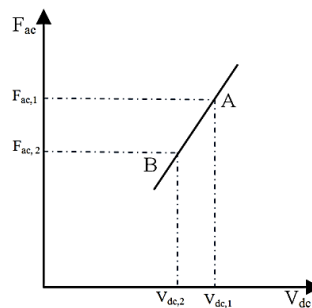


Figure 7. Effects of loads variations on voltage and frequency

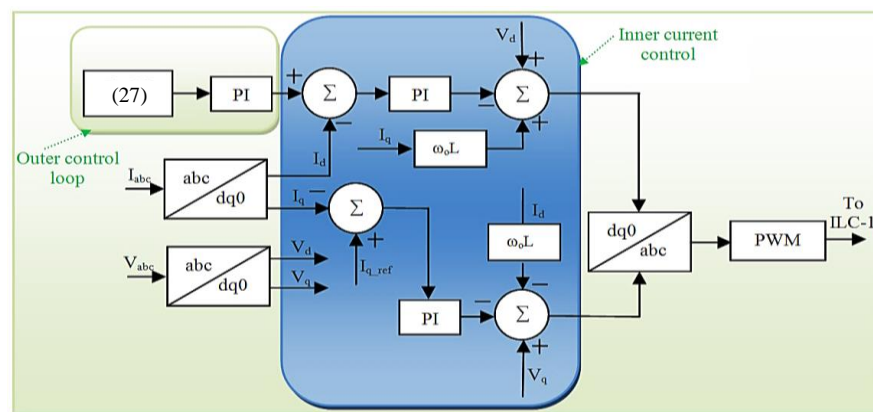


Figure 8. Proposed control scheme for ILC-1



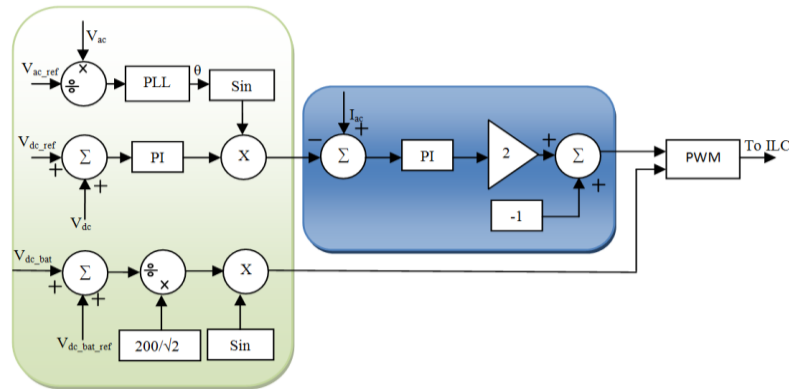


Figure 9. Proposed control scheme for ILC-2

## 5. SIMULATION RESULTS

The simulation is carried out in MATLAB/Simulink. The performance of AC/DC HMGS is discussed with different DG and ESS sources, multi terminal VSC ILC-1 and ILC-2 for three phases 380 V, 50 Hz and single phase 110 V, 220 V, 60 Hz system with efficient control schemes to extract maximum power with better power quality, double conversion converters are used for changing the frequency and control of power, buck and boost converters serving as DC-transformers for 370 V, 800 V are used for different voltage rated loads. Maximum battery SoC is set as 100% and minimum 25%, PV generates 5 KW of power, fuel cell capacity is 10 KW, and BESS capacity is linear with loads by attaching the extra battery strings. Linear loads connected with controllable switches, Separate buses on AC side and DC side are arranged which are not shown in figure to avoid complexity. PV, BESS used on AC and DC grid differs with parameter ratings, control and operating methods. The loads are segregated as critical and non-critical loads. The analysis done is on selected loads for demonstration of ILC performance.

At  $t = 0$  sec the AC grid generates 15 KW, the initial connected AC load is of 20 KW which is evident to observe a 5 KW of power deficit due to which the frequency and DC voltage droops occurs, dramatically activates ILC-1 to transfer power from DC grid of 5 KW to AC load. BESS at DC side with higher SoC% shares the power to DC loads and also transfers the power to AC loads, as DC load of 10 KW is turned on initially which is observed 4 KW and 6 KW power from PV and BESS is supplied. At  $t = 1$  sec AC load of 5 KW is turned-on and no increment on DC load, the deficit power in AC load is injected by ILC-1 through DC BESS. Similarly,  $t = 2$  sec AC load of 3 KW is turned-on 2 KW of power is injected by ILC-1 and 1 KW of power is injected by adding additional strings of batteries at AC grid. The PV power generation in AC sub grid is connected to AC critical loads. Similarly, power from fuel cell is used for charging the DC-grid BESS and serving power to DC critical loads. At  $t = 3$  sec AC power generation is boosted by attaching additional strings in BESS with capability for serving AC and DC loads. A DC-load of 5 KW is turned-on since the DC battery gradually discharges and the SoC level decreases and the control schemes is designed as higher the SoC% of battery will serve the power to loads hence the change in DC loads causes change in DC voltage and AC frequency forcing converter to share power from AC grid to DC load. Similarly at  $t = 4, 5$  sec DC loads of 2 KWs is increased and power is shared from AC sub grid through ILC-1. A control scheme is designed to charge the BESS during grid connected mode and in islanded mode if BESS SoC reaches minimum, the power from fuel cell is connected to loads. During the time interval of 1-3 sec ILC-1 behaves as inverter with power as negative and for 3-6 sec ILC-1 behaves as rectifier with power as positive. The Figure 10 shows the performance of ILC-1 as inverter and rectifier, also there are no major differences in results as compared to only ILC connected to three phase system [27]. Figure 11 show the frequency variations due to load changes. Figures 12 and 13 shows the AC and DC power of loads respectively.

The other case study for ILC-2, converter is connected with AC/DC critical and non-critical loads with separate buses and control scheme, during the outages in AC/DC grid the power can be shared from AC or DC power generating station to critical loads and also by load shedding the non-critical loads with a bidirectional ILC-2. A double conversion converter is used for changing frequency. ILC has the capability of injecting power among themselves during power requirements. PV generates around 5 KW power which is supplied to DC load of 3 KW at  $t = 0$  sec and the remaining 2 KW is supplied at  $t = 1$  sec as the load of 3 KW is turned-on, 1 KW of power is transferred from AC sub grid BESS. At  $t = 2$  sec a DC load of 3 KW is turned-on the power is transferred from AC sub grid through ILC-2 during this period of 0-3 sec ILC-2 behaves as rectifier as shown in Figure 14. At  $t = 3, 4, 5$  sec single phase AC loads with 5 KW, 2 KW, 2 KW respectively are turned on and AC supplies are disconnected. Battery strings at DC-side are added to

share power to AC loads, during the period of 3-6 sec ILC-2 behaves as inverter shown in Figure 14. The complete source power to AC/DC loads is shown in Figure 15. Figures 16-18 shows the voltages for PV, PV boost converter and AC single phase voltage respectively. Similar work for optimal usage of RES has been carried out based on linear programming optimized and solver based methods [28].

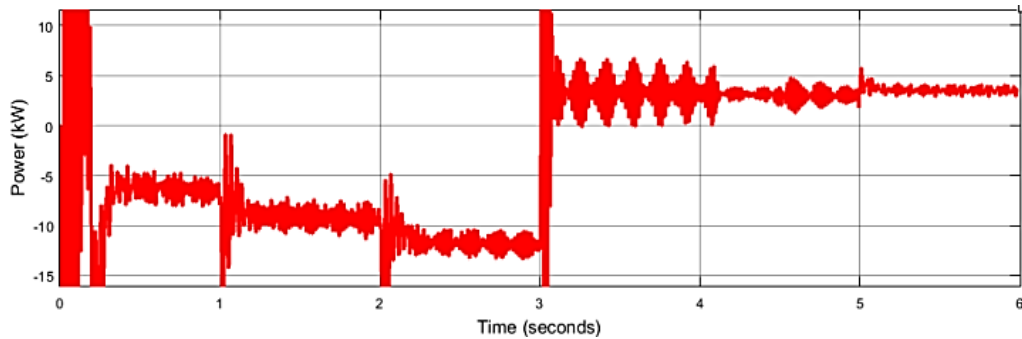


Figure 10. Performance of ILC-1 as inverter and rectifier

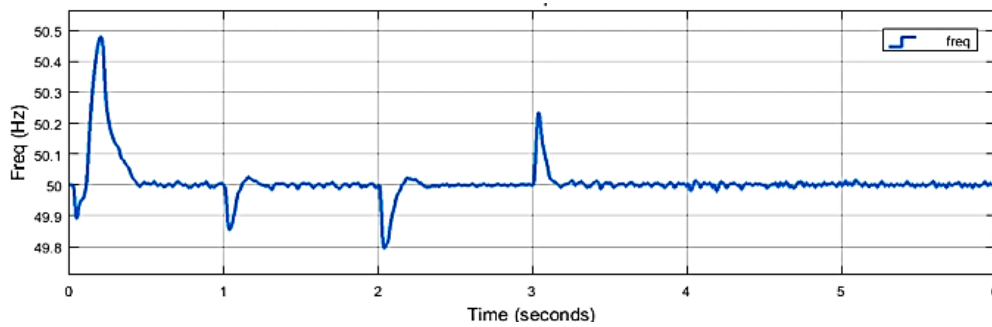


Figure 11. Frequency variations with change in loads

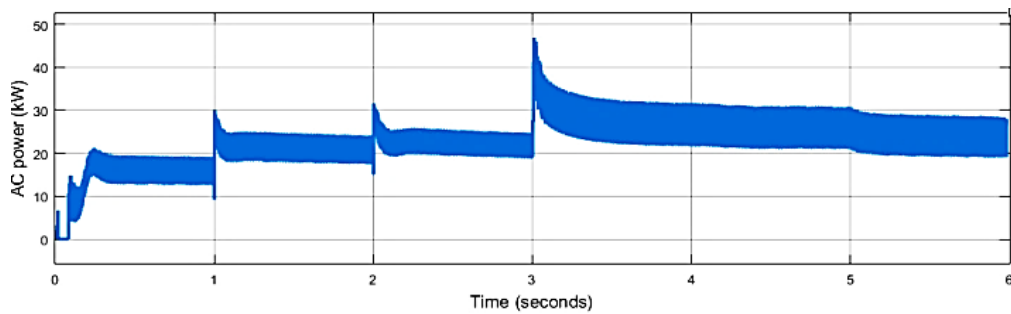


Figure 12. Power through AC loads

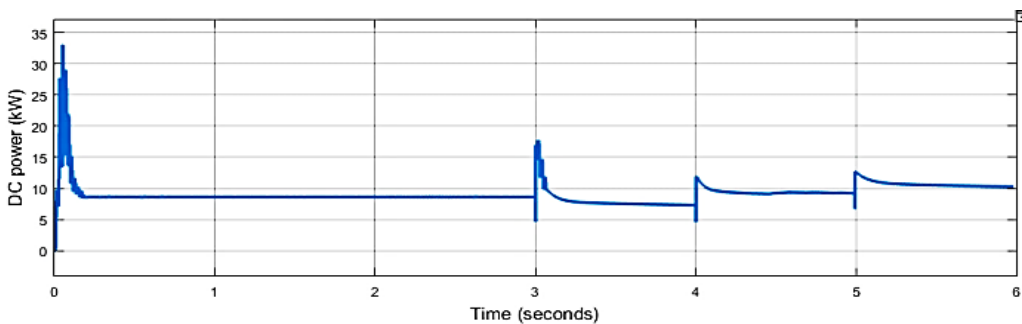


Figure 13. Power through DC loads

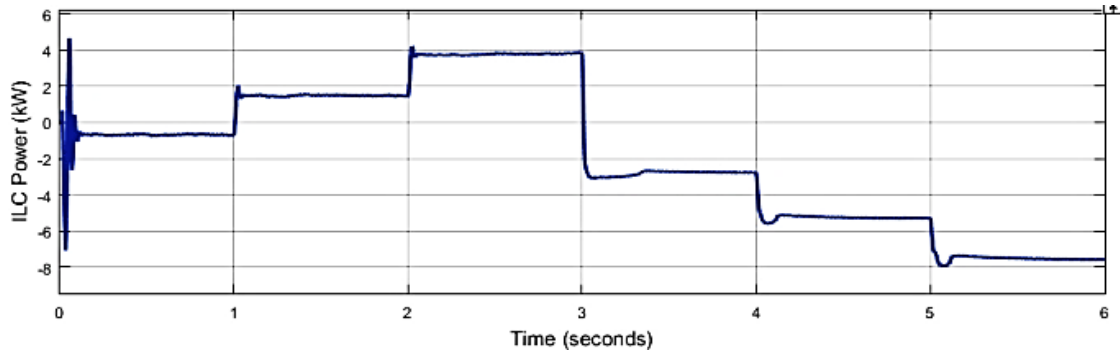


Figure 14. Performance in ILC-2 as rectifier and inverter

s

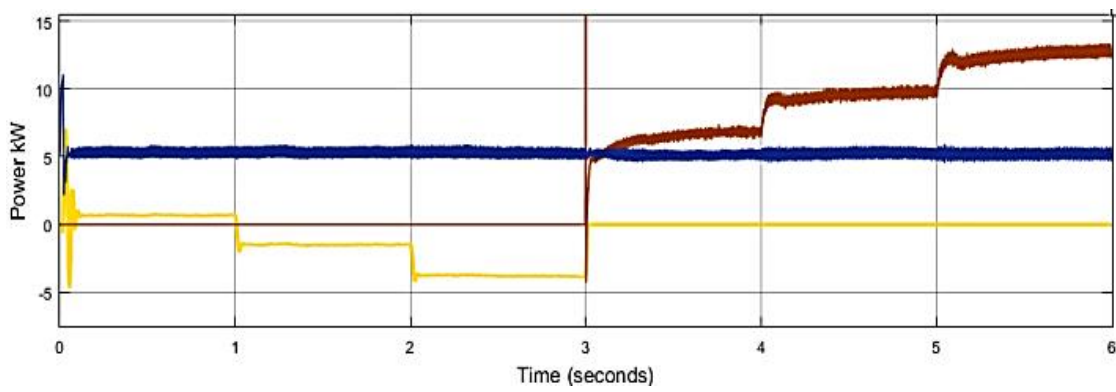


Figure 15. Powers through PV, fuel cell, and BESS

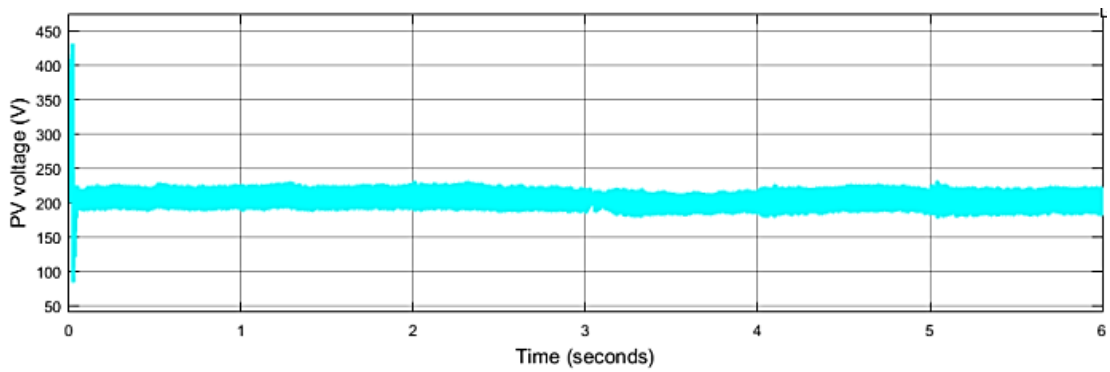


Figure 16. PV voltage

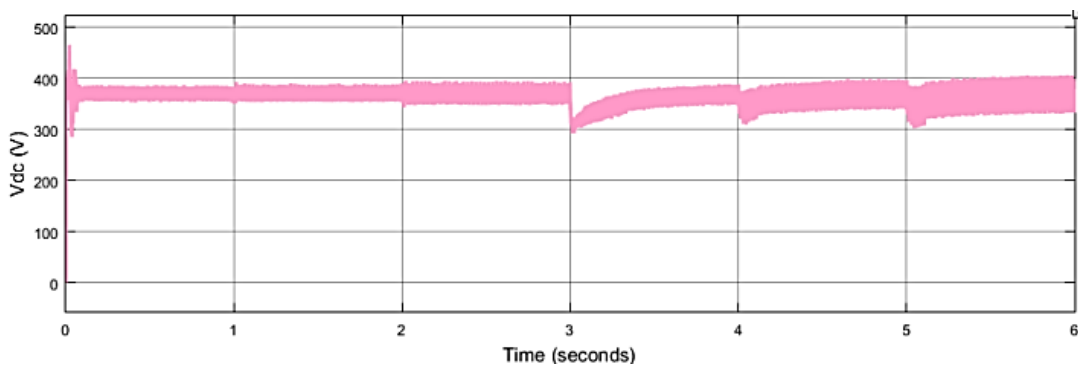


Figure 17. PV boost voltage

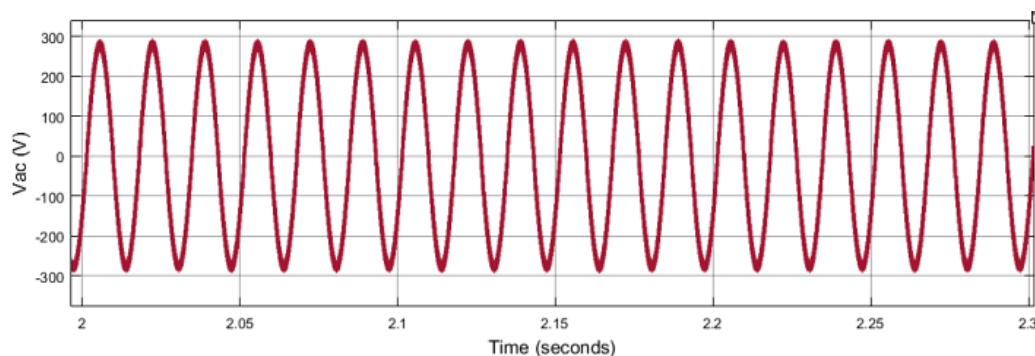


Figure 18. AC voltage

## 6. CONCLUSION

The efficient use of renewable energy sources in AC/DC hybrid micro grid interfaced with multi terminal interlinking converter for autonomous bidirectional power exchange between AC/DC sub grids is analyzed with a normalized droop control method forming an outer loop control with a simple mathematical model using DC voltage, converter power and frequency. SoC based battery control and power sharing among AC/DC loads is derived. Overall monitoring and power transfer for energy management system of critical and non-critical loads with multi interlinking converters is analyzed with change of frequency. Bidirectional DC/DC converters are used for automatic charging and discharging options.





## REFERENCES

- [1] Q. Fu, A. Nasiri, A. Solanki, A. Bani-Ahmed, L. Weber, and V. Bhavaraju, "Microgrids: architectures, controls, protection, and demonstration," *Electric Power Components and Systems*, vol. 43, no. 12, pp. 1453–1465, 2015, doi: 10.1080/15325008.2015.1039098.
- [2] A. A. Hamad, M. E. Nassar, E. F. El-Saadany, and M. M. A. Salama, "Optimal configuration of isolated hybrid AC/DC microgrids," *IEEE Transactions on Smart Grid*, vol. 10, no. 3, pp. 2789–2798, 2019, doi: 10.1109/TSG.2018.2810310.
- [3] S. K. Sahoo, A. K. Sinha, and N. K. Kishore, "Control techniques in AC, DC, and hybrid AC-DC microgrid: a review," *IEEE Journal of Emerging and Selected Topics in Power Electronics*, vol. 6, no. 2, pp. 738–759, 2018, doi: 10.1109/JESTPE.2017.2786588.
- [4] M. Naderi, Y. Khayat, Q. Shafiee, T. Dragicevic, H. Bevrani, and F. Blaabjerg, "Interconnected autonomous AC microgrids via Back-to-back converters - part I: small-signal modeling," *IEEE Transactions on Power Electronics*, vol. 35, no. 5, pp. 4728–4740, 2020, doi: 10.1109/TPEL.2019.2943996.
- [5] P. A. Gbadega and A. K. Saha, "Impact of incorporating disturbance prediction on the performance of energy management systems in micro-grid," *IEEE Access*, vol. 8, pp. 162855–162879, 2020, doi: 10.1109/ACCESS.2020.3021598.
- [6] Z. Shuai, J. Fang, F. Ning, and Z. J. Shen, "Hierarchical structure and bus voltage control of DC microgrid," *Renewable and Sustainable Energy Reviews*, vol. 82, pp. 3670–3682, 2018, doi: 10.1016/j.rser.2017.10.096.
- [7] N. H. Saad, A. A. El-Sattar, and A. E. A. M. Mansour, "A novel control strategy for grid connected hybrid renewable energy systems using improved particle swarm optimization," *Ain Shams Engineering Journal*, vol. 9, no. 4, pp. 2195–2214, 2018, doi: 10.1016/j.asej.2017.03.009.
- [8] F. Dastgeer, H. E. Gelani, H. M. Anees, Z. J. Paracha, and A. Kalam, "Analyses of efficiency/energy-savings of DC power distribution systems/microgrids: Past, present and future," *International Journal of Electrical Power and Energy Systems*, vol. 104, pp. 89–100, 2019, doi: 10.1016/j.ijepes.2018.06.057.
- [9] A. A. Ejajal, A. H. Yazdavar, E. F. El-Saadany, and M. M. A. Salama, "Optimizing the droop characteristics of AC/DC hybrid microgrids for precise power sharing," *IEEE Systems Journal*, vol. 15, no. 1, pp. 560–569, 2021, doi: 10.1109/JSYST.2020.2984623.
- [10] H. Alrajhi Alsiraji and R. El-Shatshat, "Virtual synchronous machine/dual-droop controller for parallel interlinking converters in hybrid AC–DC microgrids," *Arabian Journal for Science and Engineering*, vol. 46, no. 2, pp. 983–1000, 2021, doi: 10.1007/s13369-020-04794-y.
- [11] P. J. Chauhan, B. D. Reddy, S. Bhandari, and S. K. Panda, "Battery energy storage for seamless transitions of wind generator in standalone microgrid," *IEEE Transactions on Industry Applications*, vol. 55, no. 1, pp. 69–77, 2019, doi: 10.1109/TIA.2018.2863662.
- [12] J. Khodabakhsh and G. Moschopoulos, "Simplified hybrid AC-DC microgrid with a novel interlinking converter," *IEEE Transactions on Industry Applications*, vol. 56, no. 5, pp. 5023–5034, 2020, doi: 10.1109/TIA.2020.2996537.
- [13] X. H. T. Pham, "Power sharing strategy in islanded microgrids using improved droop control," *Electric Power Systems Research*, 2020, [Online]. Available: <https://www.sciencedirect.com/science/article/pii/S0378779619304833>
- [14] H. Saghafi and H. R. Karshenas, "Power sharing improvement in standalone microgrids with decentralized control strategy," *Electric Power Components and Systems*, vol. 42, no. 12, pp. 1278–1288, 2014, doi: 10.1080/15325008.2014.927030.
- [15] A. A. Ejajal, A. H. Yazdavar, E. F. El-Saadany, and M. M. A. Salama, "Optimizing the droop characteristics of AC/DC hybrid microgrids for precise power sharing," *IEEE Systems Journal*, vol. 15, no. 1, pp. 560–569, 2021, doi: 10.1109/JSYST.2020.2984623.
- [16] A. Vazquez, K. Martin, M. Arias, and J. Sebastian, "On bidirectional DC nano-grids: design considerations and an architecture proposal," *Energies*, vol. 12, no. 19, 2019, doi: 10.3390/en12193715.





- [17] H. Fan, W. Yu, and S. Xia, "Review of control strategies for DC nano-grid," *Frontiers in Energy Research*, vol. 9, 2021, doi: 10.3389/fenrg.2021.644926.
- [18] S. A. Razzaq and V. Jayasankar, "Autonomous power management for hybrid AC/DC nano grid using ESS and DG," *International Conference on Intelligent Controller and Computing for Smart Power, ICICCSP, 2022*, doi: 10.1109/ICICCSP53532.2022.9862413.
- [19] S. Rauf, A. R. Kalair, and N. Khan, "Variable load demand scheme for hybrid AC/DC nanogrid," *International Journal of Photoenergy*, vol. 2020, 2020, doi: 10.1155/2020/3646423.
- [20] T. Pangaribowo, W. M. Utomo, A. A. Bakar, and D. S. Khaerudini, "Battery charging and discharging control of a hybrid energy system using microcontroller," *Indonesian Journal of Electrical Engineering and Computer Science*, vol. 17, no. 2, pp. 575–582, 2019, doi: 10.11591/ijeecs.v17.i2.pp575-582.
- [21] H. J. Moon, Y. J. Kim, J. W. Chang, and S. Il Moon, "Decentralised active power control strategy for real-time power balance in an isolated microgrid with an energy storage system and diesel generators," *Energies*, vol. 12, no. 3, 2019, doi: 10.3390/en12030511.
- [22] A. Ordone, E. Unamuno, J. A. Barrena, and J. Paniagua, "Interlinking converters and their contribution to primary regulation: a review," *International Journal of Electrical Power and Energy Systems*, vol. 111, pp. 44–57, 2019, doi: 10.1016/j.ijepes.2019.03.057.
- [23] S. M. Sharkh, M. A. Abusara, G. I. Orfanoudakis, and B. Hussain, "Power electronic converters for microgrids," *Power Electronic Converters for Microgrids*, vol. 9780470824030, pp. 1–293, 2014, doi: 10.1002/9780470824054.
- [24] Y. Zahraoui *et al.*, "Energy management system in microgrids: a comprehensive review," *Sustainability (Switzerland)*, vol. 13, no. 19, 2021, doi: 10.3390/su131910492.
- [25] A. Eisapour-Moarref, M. Kalantar, and M. Esmaili, "Power sharing in hybrid microgrids using a harmonic-based multidimensional droop," *IEEE Transactions on Industrial Informatics*, vol. 16, no. 1, pp. 109–119, 2020, doi: 10.1109/TII.2019.2915240.
- [26] P. Zafari, A. Zangeneh, M. Moradzadeh, A. Ghafouri, and M. A. Parazdeh, "Various droop control strategies in microgrids," *Power Systems*, pp. 527–554, 2020, doi: 10.1007/978-3-030-23723-3\_22.
- [27] S. A. Razzaq and V. Jayasankar, "Autonomous power sharing for AC/DC HMGS using decentralized modified droop method for interlinking converter," *International Journal of Power Electronics and Drive Systems*, vol. 13, no. 4, pp. 2139–2147, 2022, doi: 10.11591/ijpeds.v13.i4.pp2139-2147.
- [28] E. I. El-Sayed, M. M. Al-Gazzar, M. S. Seif, and A. M. A. Soliman, "Energy management of renewable energy sources incorporating with energy storage device," *International Journal of Power Electronics and Drive Systems*, vol. 13, no. 2, pp. 883–899, 2022, doi: 10.11591/ijpeds.v13.i2.pp883-899.

## BIOGRAPHIES OF AUTHORS



**Syed Abdul Razzaq**     is a Research Scholar in Electrical and Electronics Engineering Department at Vel-Tech Rangarajan Dr.Sagunthala R&D Institute of Science and Technology, Chennai, India. He received his B.Tech. M.Tech. Degrees in Electrical and Electronics Engineering and Power Electronics from University Jawaharlal Nehru Technology. His research interests include the field of HMGS, Smart Grid & Micro Grid, Power Electronics, BESS, Battery Chargers, Inverters, Renewable Energy, Data Centers, Data Center Infrastructure Management, Industrial Automation and Sub-Station Automation. He can be contacted at email: vtd516@veltech.edu.in.



**Vairavasamy Jayasankar**     is Prof. in Electrical & Electronic Engineering Department and Dean-School of Electrical and Communication, Vel-Tech Rangarajan Dr. Sagunthala R&D Institute of Science and Technology, Chennai, India. He has completed his Ph.D from Anna University. He has vast experience in academics; he has published several papers in reputed journals, national and international conferences. His research of interest is in High Voltage Engineering, Power System Voltage Stability, Power Electronic Converters and Renewable Energy Sources. He can be contacted at email: deansoe@veltech.edu.in.